



Observational study of factors influencing the dispersion of warm fog droplet spectrum in Xishuangbanna, China

Zhenya An^{1,2}, Xiaoli Liu^{1,2*}

¹China Meteorological Administration Aerosol-Cloud and Precipitation Key Laboratory, Nanjing University of Information Science and Technology, Nanjing 210044, China.

²College of Atmospheric Physics, Nanjing University of Information Science and Technology, Nanjing 210044, China

Correspondence to: Xiaoli Liu (liuxiaoli2004y@nuist.edu.cn)

Abstract. The microphysical characteristics of fog and stratiform clouds are somewhat similar. The study of the microphysical characteristics of warm fog, fog droplet spectral relative dispersion, and their influencing factors can deepen our understanding of the variability and influencing factors of cloud droplet spectral relative dispersion, while also investigating the formation and maintenance mechanisms of fog. This is currently a scientific issue that still remains controversial in cloud physics research and climate prediction. In this paper, we analyzed three months of Xishuangbanna radiation fog observations to explore the microphysical characteristics of fog. The results show followings: (1) When the autoconversion threshold (T) increased to greater than 0.4, the positive correlation between the relative dispersion of fog droplet spectrum and the volume mean diameter or water content of fog droplet weakened, also the positive correlation between relative dispersion and number concentration increased where the main mechanism needed to be integrated considering the interaction of collision-coalescence, condensation, and nucleation processes. It is found that the strength of the collision-coalescence process has a certain influence on the variation rule of dispersion. (2) The number concentration of 2-12 μm droplets in the fog constrained the relationship between the T and relative dispersion, with the number of large droplets reflects the strength of the collision-coalescence process. (3) Supersaturation changed microphysical quantities by increasing the number concentration of small droplets in the fog, which affected the variations of relative dispersion. For supersaturation greater than 0.12 %, the number concentration of droplets larger than 30 μm may be decreased due to gravitational settling. In addition, there is no significant relationship between supersaturation and relative dispersion if the initial nucleated fog droplet spectrum is narrow .

1 Introduction

Fog is a common weather phenomenon where water vapor condenses (or freezes) and suspends in the atmospheric boundary layer near the Earth's surface, causing visibility to be less than 1 km. The existence of fog can easily lead to road traffic accidents. Although drivers face meteorological disasters such as ice, snow, wind, and fog on the road, ice, snow, and wind can be accurately predicted and reduced in harm through sanding, snow removal machines, as well as designing road sections and bridge structures (Musk, 1991). However, due to the complex formation mechanism and variable atmospheric background, it is very difficult to forecast the intensity of fog. The economic losses related to fog and low visibility are even comparable to



those caused by other weather events such as tornadoes and hurricanes (Gultepe et al., 2007). Therefore, the impact of fog on transportation has gradually been given more attention. In addition, the temperature inversion structure during fog formation is also unfavorable for the diffusion of pollutants, seriously affecting air quality. Fog itself also has a certain self-purification effect on the atmosphere, but when the concentration of pollutants in the atmosphere exceeds the self-purification capacity of the atmosphere, it will cause atmospheric pollution. Therefore, research on formation mechanism and microphysical characteristics of fog is conducive to deepening people's scientific understanding, thereby improving the accuracy of fog forecasting.

In the autumn of 1959, Okita (1962) used balloons to measure the distribution of fog droplet number concentration and liquid water content with height in mountain fog in Hokkaido, Japan. In 1970, NASA supported the Cornell Laboratory (CAL) to conduct field observation experiments in New York for the purpose of artificial fog elimination, obtaining the vertical structure of fog microphysical characteristics (Pilié et al., 1975). The earliest fog observation experiment in China took place in Shanghai (Li, 2001). In 1968 and 1969, a fog census was also conducted in the southern provinces of China, and preliminary observations of fog microstructure were made in Yunnan, Guizhou, and Sichuan (Niu et al., 1989). Niu et al. (2010) investigated the microphysical characteristics of persistent fog, using experimental data from fog observations in Pancheng town, a northern suburb of Nanjing, in winter 2006. Yang et al. (2021) used the microphysical observation data of the Tianjin radiation fog in the winter of 2016/2017 combined with meteorological tower data to reveal the observation facts of the microphysical and size distribution characteristics of fog droplets and discuss fog formation and dissipation mechanisms. Wang et al. (2021) elaborated the physical and chemical characteristics of radiation fog using observation data from December 2019 to February 2020 in the tropical rainforest area of Xishuangbanna.

Given the above, the microphysical characteristics investigation occupies an important position in the study of fog. The relative dispersion is an important physical quantity of the fog microphysical characteristics, and it is a parameter that describes the degree of relative dispersion of the fog droplets size distribution. Besides, the relative dispersion of cloud (fog) droplet spectrum has been the focus of research in cloud physics for the last two decades (Desai et al., 2019), which can also influence the fog lifetime by affecting the autoconversion threshold function (T) (Lu et al., 2021). It is crucial for the accurate description of cloud droplet microphysics in weather and climate model. Many observational experiments on relative dispersion have been carried out worldwide (Zhao et al., 2006; Berg et al., 2011). Lots of meteorologists have explored the relationship between the relative dispersion and microphysical quantities. For example, Liu and Daum (2002), Rogers and Yau (1989), Yum and Hudson (2005) used condensation theory to predict that relative dispersion would increase with increasing of cloud droplet number concentration. However, observations have also shown that the relationship between relative dispersion and number concentration is not simply a monotonic increasing or decreasing relationship. It is shown that relative dispersion decreases with increasing number concentration (Lu et al., 2007, 2012; Miles et al., 2000; Pawlowska et al., 2006; Wang et al., 2009). The relationship between relative dispersion and number concentration can also affect the aerosol first effect by changing the



65 effective radius of cloud droplets (Liu et al., 2002; Lu et al., 2021). Zhao et al. (2006) found that relative dispersion of cloud
droplets gradually converges as the number concentration increases. In addition to the correlation with number concentration,
there is also a correlation between the relative dispersion and the mean-volume diameter of cloud droplet, which determines
the effect of relative dispersion on the Twomey effect (Wang et al. 2023), while the correlation between the two should also
70 and found a positive correlation between relative dispersion and mean-volume diameter. However, it has also been shown that
there is a negative correlation between these two as well (Liu and Daum, 2002; Anki et al., 2016).

Therefore, numerous factors influence the relative dispersion evolution, and its evolution pattern has great uncertainty, which
makes the study of cloud and fog microphysics difficult. It has been investigated that droplet collision-coalescence processes
75 may also have an impact on the spectral dispersion and its evolutionary pattern on the basis of droplet nucleation and
condensation growth. With the T-value is an important parameter for measuring the automatic transformation from cloud to
rain droplet, its numerical magnitude indirectly indicates the strength of the collision-coalescence process in clouds and fog
(Liu et al., 2005,2006). This paper intended to analyze the fog micro-physical characteristics and relative dispersion
characteristics in conjunction with T-value, background aerosol and supersaturation evolutions, so as to deepen the scientific
80 understanding of the fog micro-physical properties.

2 Methods

2.1 Introduction of field observation

In the winter of 2019 (November 22, 2019 to February 28, 2020), the fog research team of the NUIST and researchers in the
Key Laboratory of Tropical Forest Ecology conducted a comprehensive field detection experiment in the tropical rainforest
85 area of Xishuangbanna, China. This work used data sampled by the Fog Monitor in model 120 (FM-120) from the Droplet
Measurement Technologies (DMT) and A 1000XP Wide-Range Particle Spectrometer (WPS-1000XP, MSP Corporation,
USA) during the experiment. Different from FM-100 (Spiegel et al., 2012), the measurement range of the FM-120 is 2-50
 μm with a sampling frequency of 1 Hz, hence no data exclusion processing was required for the first bin. The WPS-1000XP
measures the aerosol number-size distribution ($N_a(D)$) with diameter ranging from 10 nm to 10 μm divided into 120 bins and
90 completes a full spectrum sample every 6 minutes. Due to the lack of visibility observations, this article referred to cloud
criteria, using a number concentration greater than 10 cm^{-3} and a water liquid content greater than or equal to 0.001 g m^{-3} as
the fog criteria, to judge whether it is a fog process from a microphysical perspective (Wang et al., 2021; Lu, et al. 2013).



2.2 Calculation

2.2.1 microphysical quantities in fog

95 Based on the fog droplet spectrum ($N_f(D)$) measured by FM-120, the number concentration of fog droplets (N_f), mean arithmetic diameter (MD), mean-volume diameter (MVD), liquid water content (LWC), standard deviation of droplet spectrum (σ), and relative dispersion (ε) were calculated. Where D denotes the droplet diameter of each bin. The calculation formulas are as follows:

$$N_f = \sum_{D_i}^k \frac{N_f(D_i)}{PAS \cdot S \cdot \Delta t}, \quad (1)$$

100 $MD = \frac{\int N_f(D) \times D \, dD}{N_f}, \quad (2)$

$$MVD = \left(\frac{\int N_f \times D^3 \, dD}{N_f} \right)^{\frac{1}{3}}, \quad (3)$$

$$LWC = \int \frac{\pi}{6} \rho_w \times N_f(D) \times D^3 \, dD, \quad (4)$$

$$\sigma = \left(\int N_f(D) \times (D - MD)^2 \, dD / N_f \right)^{1/2}, \quad (5)$$

$$\varepsilon = \frac{\sigma}{MD}, \quad (6)$$

105 Where, $k = 30$, PAS is the airflow velocity in m s^{-1} , S is the sampling area in mm^2 , t is the sampling frequency, and the integration range of the above equation is from 2 to 50 μm . At the same time, in order to eliminate the influence of instrument noise on the acquired data, the FM-120 droplet spectrum information was averaged for 1 min in this paper.

Since aerosols complete a full spectrum sampling every 6 min, each aerosol particle data was considered to represent the average state within 6 min for the calculation. In order to combine the aerosol data with the fog data for analysis, the fog data within one aerosol sampling time were therefore averaged, and the individual microphysical quantities in the fog were recalculated.

2.2.2 Visibility

For facilitating the study of fog classification, the visibility data in fog observed in Xishuangbanna in this paper were calculated using the $N_f(D)$ information. The visibility and extinction coefficients were calculated as follows.

$$V = \frac{-\ln \alpha}{\beta}, \quad (7)$$

In the above equation,



$$\beta = \pi \sum_{i=1}^k Q_{ext} n_i(r_i) r_i^2, \quad (8)$$

Among them,

$$120 \quad Q_{ext} = 2 - \frac{4}{\rho} \sin \rho + \left(\frac{2}{\rho}\right)^2 (1 - \cos \rho), \quad (9)$$

In the above equation, α is the contrast threshold, usually equal to 0.02. β is the extinction coefficient in km^{-1} . Q_{ext} is the meter scattering coefficient. r_i is the radius of the i -th fog droplet. $n_i(r_i)$ is the fog droplet number concentration at the radius. Where $\rho = 2x(m - 1)$, for water droplets $m=0.75$. And r is the radius, which is usually considered to be 0.5.

2.2.3 Supersaturation

125 Based on the calculation method of Petters and Kreidenweis (2007), Shen et al. (2018) and Mazoyer et al. (2019), since droplets are the product of aerosol activation under specific supersaturation conditions, the supersaturation (SS) can be calculated indirectly with known information about aerosols and droplets.

$$D_c = \left(\frac{3kD_a^3}{A}\right)^{\frac{1}{2}}, \quad (10)$$

Where,

$$130 \quad A = \frac{4\sigma_s M_w}{RT_{em}\rho_w}, \quad (11)$$

In the above equation, $\sigma_{s/a}$ is the droplet surface tension (assumed to be pure water, 0.0728), M_w is the molar mass of water, R is the gas constant, T_{em} is the ambient atmospheric temperature measured in real time using FM-120, D_c is the diameter of the activated droplet, and D_a is assumed to be the critical activation diameter of the dry aerosol. Referring to measurements of aerosol hygroscopicity in the Amazon rainforest region (Pöschl et al., 2010; Wang et al., 2021), k was assumed to be 0.15.

135 where A can be simplified (Seinfeld and Pandis, 2016) as,

$$A \cong \frac{0.66}{T_{em}}, \quad (12)$$

A as a function of temperature T_{em} in μm . D_a was calculated by referring to Wang et al.(2021). The calculation of D_a was done by making a cycle from large to small with the central diameter D_a of each of the 120-bin aerosol spectra, finding the two D_a corresponding to when the integration of the droplet spectrum concentration in the previous cycle was larger than the
 140 integration of the aerosol spectrum concentration, and when the opposite sign was in the next cycle, and obtaining the integration when it is equal by interpolation, and after calculating, the corresponding of D_c , so that the supersaturation SS_c can be calculated, thereby obtaining D_a and its corresponding D_c . Finally, according to the reciprocal relationship between the critical $SS(SS_c)$ and D_c .



$$SS_c = \frac{200A}{3D_c}, \quad (13)$$

145 2.2.4 Autoconversion threshold function

In order to study the collision-coalesces process in fog, an autoconversion threshold function (T) was introduced. T is an important microphysical quantity describing the intensity of the collision-coalesces between droplets within clouds and fog. The calculation derived by Liu et al. (2005) as follows:

$$T = \frac{P}{P_0} = \frac{\left[\int_{r_c}^{\infty} r^6 n(r) dr \right]}{\left[\int_0^{\infty} r^6 n(r) dr \right]} \frac{\left[\int_{r_c}^{\infty} r^3 n(r) dr \right]}{\left[\int_0^{\infty} r^3 n(r) dr \right]}, \quad (14)$$

150 where r is the radius of the droplet, b is the number of cloud droplets per unit volume per unit radius, and r is the critical radius of the T . the analytical expression derived by Liu et al. (2004) is as follows:

$$r_c \approx 4.09 \times 10^{-4} \beta_{con}^{\frac{1}{6}} \frac{N_f^{\frac{1}{6}}}{LWC^{\frac{1}{3}}}, \quad (15)$$

$\beta_{con} = 1.15 \times 10^{23} \text{ s}^{-1}$, is an empirical constant. T varies from 0 to 1, with larger values of T indicating higher collection efficiency.

155 3 Results and analysis

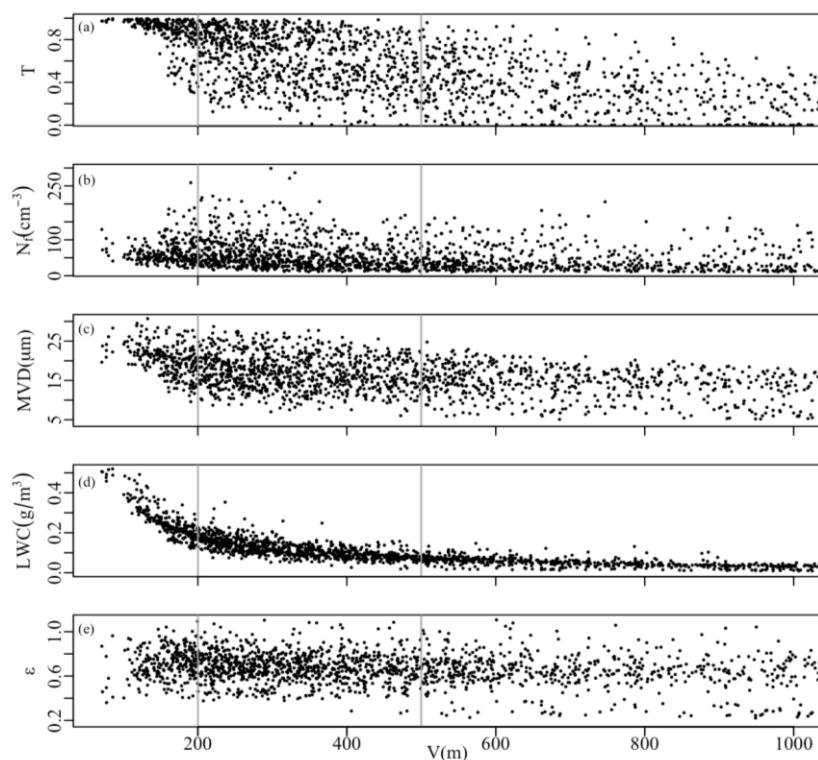
Based on the start and end times of the 19 fog events measured during the XSBN-FOG-2019 experiment. These 19 fog events have typical radiation fog characteristics (Wang et al., 2021). Referring to the national standard “Fog Forecasting Level” (General Administration of Quality Supervision, Inspection and Quarantine of the People’s Republic of China and China National Standardization Management Committee, 2012), fog was classified according to visibility. Table 1 shows the average values of different microphysical characteristics for fog with different visibility. The average value of T for the 19 fog samples was 0.38, N_f was 48.55 cm^{-3} , LWC was 0.078 g m^{-3} , ε was 0.56. As the fog intensity increased, all physical quantities increased. As shown in Fig. 1, T , N_f , MVD , and LWC all increased as V decreased.

Figure 2 shows the relationship between the fog microphysical quantities and the fog time percentage for the 19 fog processes. The proportion of fog time indicates the fog time as a percentage of the overall process duration, and a larger proportion indicates a more continuous fog. N_f , LWC , MVD , and ε all increase with increasing fog time percentage. This is due to the fact that when the fog is more continuous, the fog persists longer and is relatively deeper.



Table 1: Mean values of fog microphysical characteristic quantities at different visibilities

Fog Types	N_f (cm^{-3})	MVD (μm)	LWC (g m^{-3})	T	ϵ
Heavy fog (500m-1000m)	44.15	14.40	0.052	0.34	0.64
Dense fog (200m-500m)	59.35	17.09	0.118	0.62	0.68
Strong dense fog (<200m)	66.65	20.23	0.256	0.86	0.72



175 **Figure 1: Variations of autoconversion threshold (T), number concentration (N_f) and volume mean diameter (MVD) of fog droplets, liquid water content (LWC), and relative dispersion (ϵ) of fog droplet spectrums with visibility (V)**

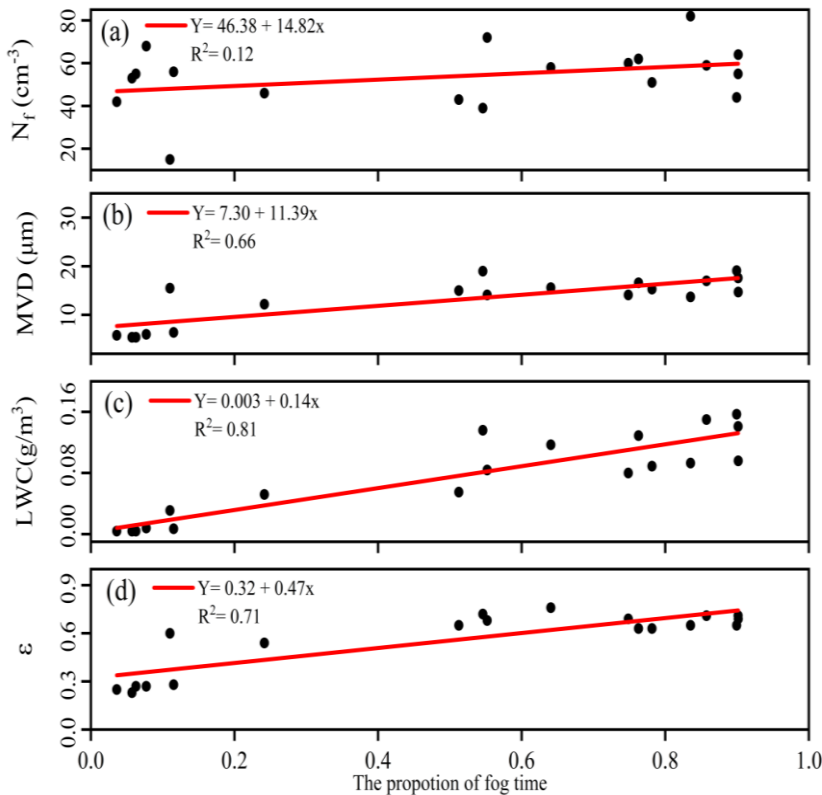


Figure 2 Variations of the mean values of number concentration (N_f) and volume mean diameter (MVD) of fog droplets, water content (LWC), and relative dispersion (ϵ) of fog droplet spectrums, with respect to the proportion of fog time, with red solid lines are linear fitted lines

180 3.1 The relationship between relative dispersion and fog microphysical characteristics

It is shown in Fig. 3a that the relationship between ϵ and MVD in fog is not a simple monotonic relationship. For MVD less than $15 \mu\text{m}$, ϵ and MVD are positively correlated, and for MVD greater than $15 \mu\text{m}$, the relationship becomes negative. Lu et al. (2020) linked the relationship between these two quantities to microphysical processes, pointing out that when MVD and ϵ are positively correlated, droplet condensation and activation processes occur simultaneously, and the changes in ϵ and MVD are consistent. When MVD is negatively correlated with ϵ , only condensation process or weak activation exists in the cloud. Therefore, if the fog droplet grows mainly through the condensation process, there is a limitation in its size growth, while the small droplets grow up by condensation process, and the weak activation of droplets leads to the small droplets cannot be replenished in time, thus the $N_f(D)$ becomes narrower and the ϵ decreases.

190 The microphysical characteristics of fog are similar to those of stratiform clouds (Wang et al., 2023), and research findings on stratiform clouds are applicable to fog droplets. In Xishuangbanna, there are differences in the relationship between ϵ and



MVD under different collision and coalescence intensities (Fig.3a) . When $T < 0.4$, ε increases and then decreases with *MVD*. When $0.4 < T < 0.8$, the decreasing trend of ε with *MVD* is significant. As T increases to above 0.8, the decreasing trend of ε with *MVD* weakens. During the fog process, not only the condensation and activation of fog droplets affect ε , but also the collision and coalescence processes between fog droplets have an impact on ε of fog spectrum, which can dominate the negative correlation between ε and *MVD*, should not be ignored.

As shown in Fig. 3b, in the context of low T values ($T \leq 0.4$), if both condensation and activation processes occur simultaneously, ε also increases with the increase of *LWC*. As shown in Fig. 4, when *MVD* is less than 15 μm , ε increases with the increase of *LWC*, with both fog droplet activation and condensation are active in this process. However, after *MVD* exceeds 15 μm , ε does not continue to increase with the increase of *LWC*, indicating a lower level of activity in the fog droplet nucleation process. This further suggests that the activation process of fog droplet weakens when *MVD* of fog droplet exceeds 15 μm .

Figure 5 shows the scatter plot of ε and N_f for different ranges of T values. From Fig. 5a and Fig. 5b, it can be seen that when T is less than or equal to 0.4, ε converges as N_f increases. However, for T values greater than 0.4, there is a tendency for ε to increase with an increase in N_f . There are two possible scenarios for a lower N_f , either the fog droplet activation is limited, or the coalescence process is more active, leading to a reduction in N_f . Therefore, in situations where the coalescence process is more active, ε decreases with a decrease in N_f .

In order to analyze in depth, the probability density of droplet size and concentration in different T value ranges were analyzed (Fig. 6). When $T \leq 0.2$, the droplets are mainly distributed in the size of less than 12 μm (Fig. 6a). When $0.2 < T < 1.0$ (Fig. 6b-e), the N_f of larger droplets increases and smaller droplets gradually decreases. As shown in Fig. 6e, for $0.8 < T \leq 1.0$, the N_f of droplets with sizes larger than 12 μm increases to the maximum, and the $N_f(D)$ widens towards the larger droplet end. The main reason may be that under larger T values, the coalescence process of droplets is active, leading to excessive consumption of smaller droplets and generation of larger droplets. It can be seen that when $T \leq 0.4$, there are generally not many large droplets, and the growth of N_f mainly relies on the nucleation process to increase the N_f of smaller droplets, resulting in slow condensation growth and a relatively narrow $N_f(D)$. When $T > 0.4$, the coalescence between droplets increases the occurrence probability of large droplets, and the consumption rate of small droplets accelerates. Therefore, increasing the N_f is beneficial to broaden the $N_f(D)$ in this situation, and there is a positive correlation between ε and N_f .

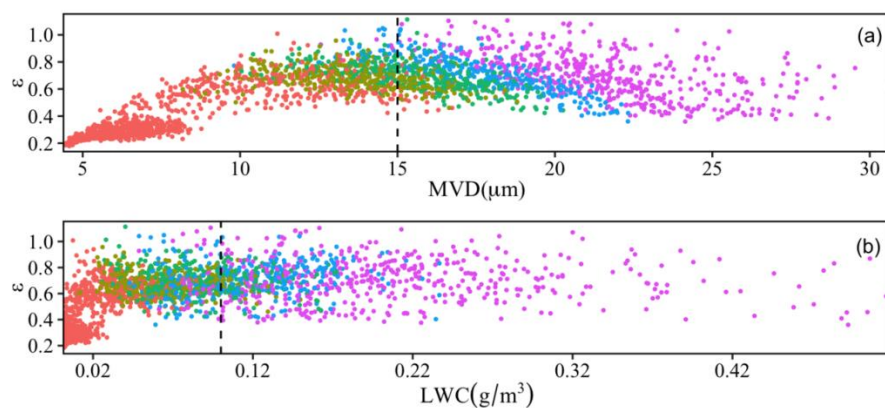


Figure 3: Variation of relative dispersion (ϵ) with volume mean diameter (MVD) and liquid water content (LWC),

(a) black dashed line for $MVD=15 \mu\text{m}$; (b) black dashed line for $LWC=0.1 \text{ g m}^{-3}$

225

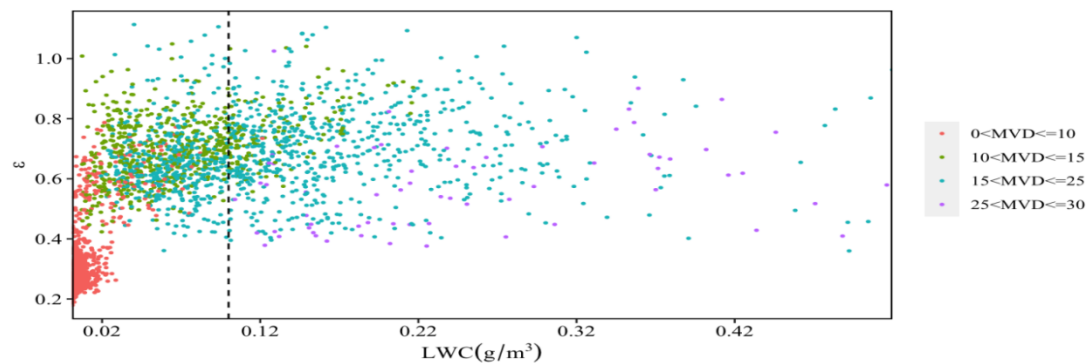
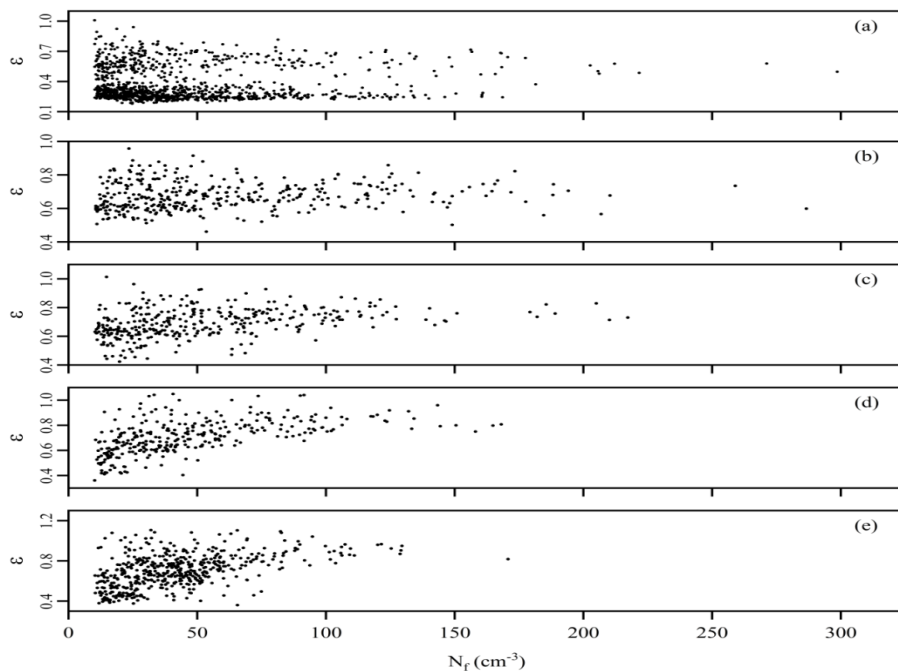
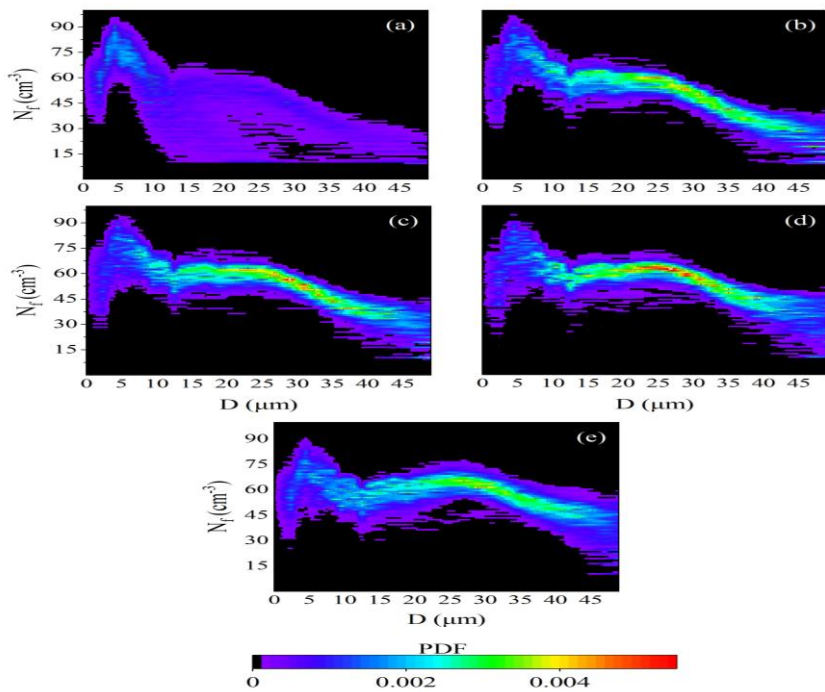


Figure 4: Relationship between water content (LWC) and relative dispersion (ϵ) (black dashed line $LWC=0.1 \text{ g m}^{-3}$)



230

Figure 5: Scatter plot of relative dispersion (ε) versus number concentration (N_f) for (a) $T \leq 0.2$; (b) $0.2 < T \leq 0.4$; (c) $0.4 < T \leq 0.6$; (d) $0.6 < T \leq 0.8$; (e) $0.8 < T \leq 1.0$





235 **Figure 6: Fog droplet particle size, concentration probability density function (a) $T \leq 0.2$; (b) $0.2 < T \leq 0.4$; (c) $0.4 < T \leq 0.6$;
(d) $0.6 \leq T < 0.8$; (e) $0.8 < T \leq 1.0$**

3.2 Relationship between T value and fog microphysical quantities

As mentioned earlier, T reflects the activity of the collision-coalescence of fog droplets. In the low T -value background, there is a limitation of particle size increase due to droplet condensation, resulting in narrower droplet spectrums. As T increases, the collision-coalescence process of fog droplets becomes more and more active, so the ε may be affected by the nucleation, condensation, and coalescence processes of fog droplets. Therefore, it is necessary to consider the evolutions of T in fog process.

Figure 7a and b show that T has an increasing and then constant relationship with MVD and LWC . The relationship between T and LWC indicates that the strength of the coalescence process is determined by the condition of the fog droplet condensation process. Condensation growth leads to a broadening of the fog droplet spectrum and the occurrence of the coalescence process. A larger MVD makes the coalescence process more likely to occur. However, there are still differences in the increasing trend of T with LWC and MVD . When MVD is small, the rate of increase in T is slower, indicating that during this stage, the condensation growth gradually allows the coalescence process to occur and become active. In the later stage, with the occurrence of the coalescence process, MVD increases rapidly, further enhancing the coalescence process.

250 Compared to MVD and LWC , the relationship between T and N_f or ε is relatively complex. When N_f is less than or equal to 100 cm^{-3} , there is no significant relationship between T and N_f . However, when N_f is greater than 100 cm^{-3} , T tends to decrease with an increase in N_f . The enhancement of the coalescence process has a negative effect on N_f , which is related to the interaction between the coalescence, and activation-condensation of fog droplets. If the former is stronger than the latter, the N_f decreases, and vice versa, the N_f increases. However, if their effects cancel each other out, in the absence of other external forces, the N_f remains unchanged. Thus, low values of N_f may correspond to different situations, which may be one of the main reasons why T values are not significantly related to them when N_f is less than 100 cm^{-3} .

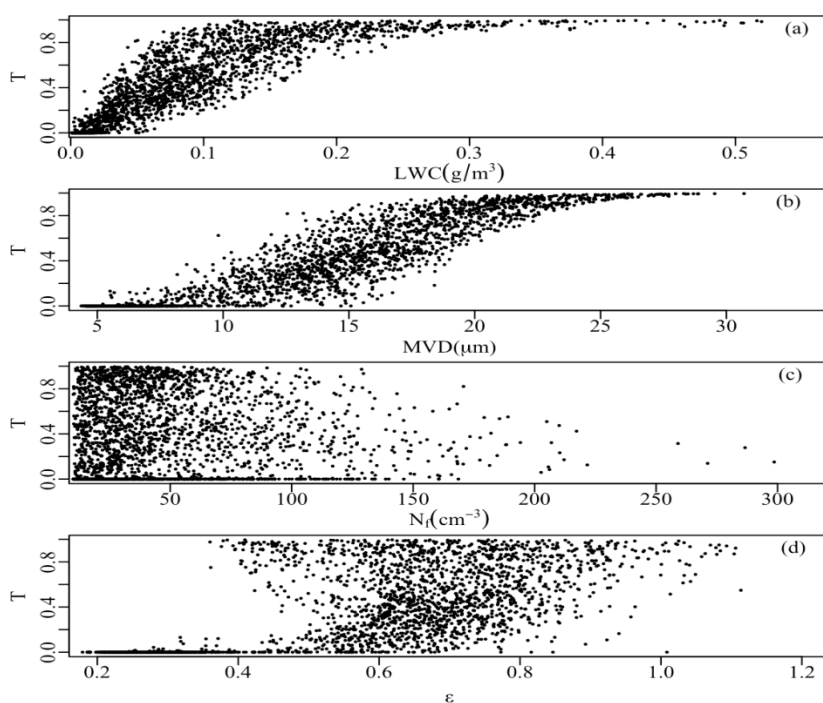
260 According to Fig 7d, When $\varepsilon \leq 0.4$, T is generally less than 0.1. When $\varepsilon > 0.4$, T initially increases with ε and then begins to spread towards larger and smaller values. The larger the T , the more obvious the spreading phenomenon. To further analyze the relationship between T and ε , the concentration and size probability density distribution of fog droplets with different T and ε are analyzed (Fig. 8).

265 Combining the relationship between ε and T in Fig 7d, as shown in Fig 8, the relationship of $\varepsilon - T$ in $T > 0.4, 0.4 < \varepsilon \leq 0.7$ (Fig. 8c) is negative, and the rest are positive. For $T > 0.4, 0.4 < \varepsilon \leq 0.7$, the N_f of $2 \sim 12 \mu\text{m}$ significantly smaller than the other cases. The reason for this may be that the collision-coalescence process is active and the nucleation process cannot



replenish the small droplets consumed by the collision-coalescence process in time, and the $N_f(D)$ will broaden toward the large droplet end, so the stronger the collision-coalescence process is, the smaller the ε is.

270 As can be seen from Fig. 8c and f, even with the same range of T values, there is a significant variation in the ε in which may be related to the aerosol concentration in the environment where the instrument was located (Chandrakar et al., 2018). It is evident that a larger ε corresponds to a wider range and higher probability of particle number concentrations greater than 12 μm . At the same time, a lower N_f in the range of 2-12 μm may likely result in lower ε of the fog (Fig. 8d).



275 **Figure 7: Scatter plot of autoconversion threshold (T) and water content (LWC), volume mean diameter (MVD), number concentration (N_f), relative dispersion (ε)**

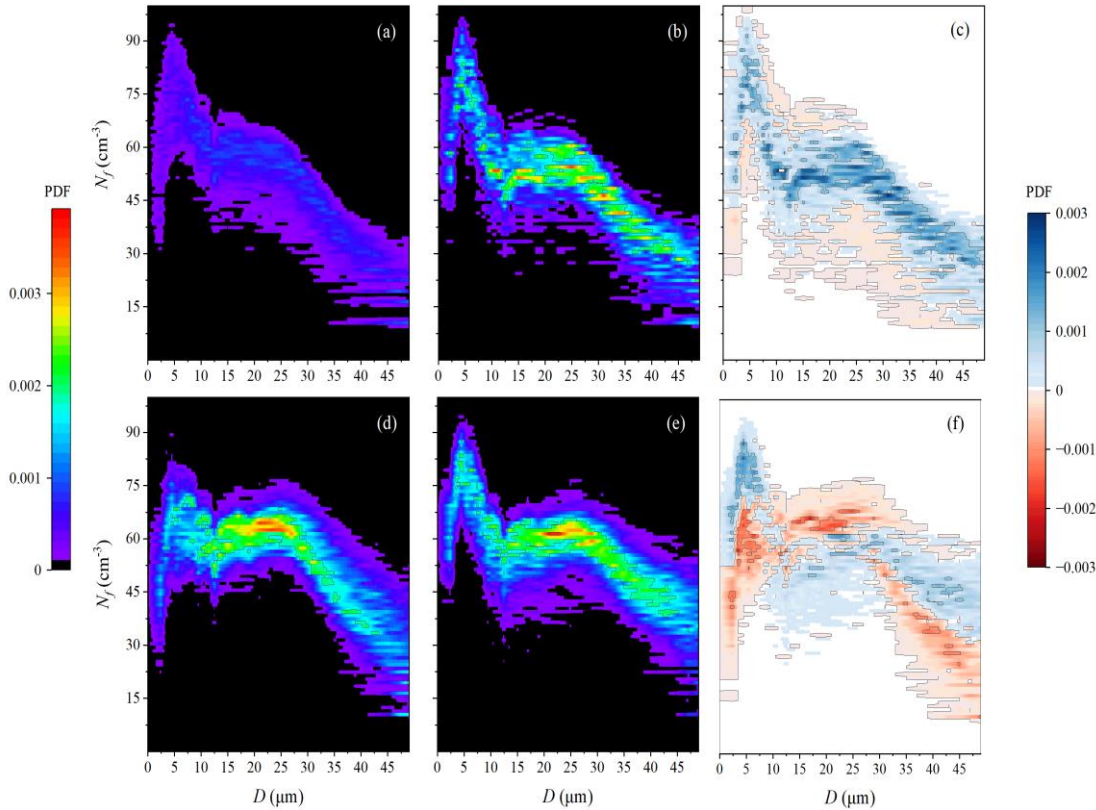


Figure 8: Probability density function of fog droplet size and concentration for (a) $T \leq 0.4, 0.4 < \varepsilon \leq 0.7$; (b) $T \leq 0.4, \varepsilon > 0.7$; (c) difference of $T \leq 0.4, \varepsilon > 0.7$ and $T \leq 0.4, 0.4 < \varepsilon \leq 0.7$; (d) $T > 0.4, 0.4 < \varepsilon \leq 0.7$; (e) $T > 0.4, \varepsilon > 0.7$; (f) difference of $T > 0.4, \varepsilon > 0.7$ and $T > 0.4, 0.4 < \varepsilon \leq 0.7$

In summary, the correlation between ε and T is related to the N_f in the range of $2 \mu\text{m}$ to $12 \mu\text{m}$. The coalescence process can reduce the number of small droplets and broaden the droplet spectrum towards the larger droplet end. If the smaller droplets are not replenished, ε decreases with increasing T , whereas ε and T are positively correlated when the smaller droplets are replenished. Although ε is related to T , high ε values can still exist in the background of low T values, and similarly, low ε values can exist in the background of high T values, both of which are related to the activation of fog droplet at the location.

In addition, the occurrence probability and $N_f(D)$ of fog droplets with diameters from $20 \mu\text{m}$ to $28 \mu\text{m}$ reflect the magnitude of T from a lateral perspective. A higher N_f value for fog droplets with diameters ranging from $20 \mu\text{m}$ to $28 \mu\text{m}$ indicates a stronger T value.

3.3 Relationship between supersaturation and fog microphysical characteristics

Under atmospheric supersaturation conditions, aerosol particles can be activated and form fog droplets, thereby indirectly affecting the ε . In this study, the SS obtained from the dry aerosol spectrum will be used to analyze its impact on fog characteristics. The fog droplet concentration increases with increasing SS (Fig. 9a).

As shown in Fig. 9b, when the MVD is less than $10\ \mu\text{m}$, there is no significant correlation between SS and MVD . However, when MVD is greater than $10\ \mu\text{m}$, MVD increases initially and then decreases with increasing SS . Based on Fig. 9c and Fig. 9e, it can be seen that LWC and T also exhibit similar relationships with SS . The average value of D_a , calculated by taking into account the ε less than or equal to 0.4, is approximately $0.3\ \mu\text{m}$. For ε greater than 0.4, the average value of D_a is approximately $0.25\ \mu\text{m}$. Therefore, the larger the aerosol activation particle size, the narrower the fog droplet spectrum, resulting in a small ε that does not vary much with SS . As shown in Fig. 9d, there is no significant relationship between SS and ε when $\varepsilon \leq 0.4$. However, when $\varepsilon > 0.4$, ε initially increases and then decreases with SS .

From Fig. 10, it can be seen that as SS increases, the $N_f(D)$ of fog droplets smaller than $10\ \mu\text{m}$ increases. As SS increases, the ε increases due to the combined effects of cloud droplet condensation growth and activation. With further increases in SS , the activation of droplets intensifies, leading to a decrease in the MVD of the droplets. What's more, when SS exceeds 0.12 %, the N_f of fog droplets in the range of $30\ \mu\text{m}$ to $50\ \mu\text{m}$ decreases, may also due to gravity settling, leading to a decrease in MVD and LWC , and subsequently a decrease in T .

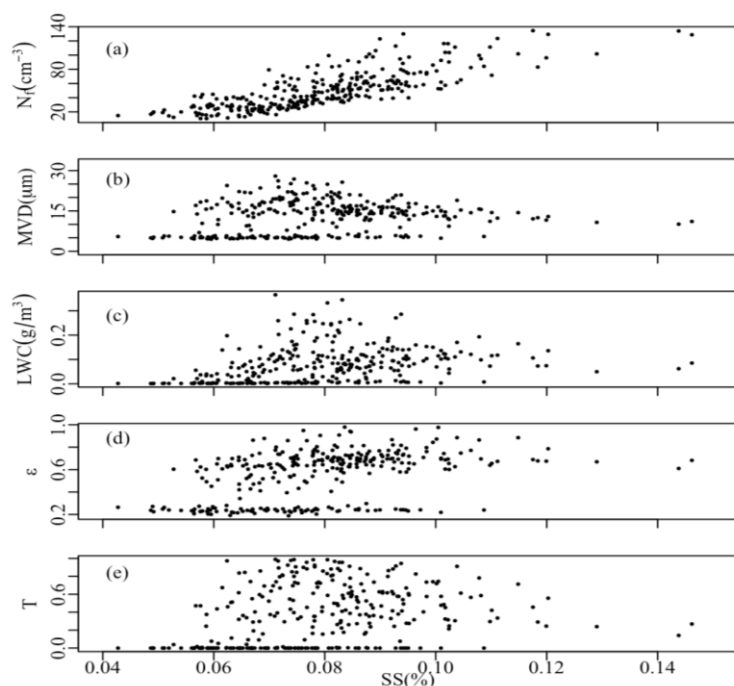




Figure 9: Scatter plots of supersaturation (SS), number concentration (N_f) and volume mean diameter (MVD) of fog droplet, water content (LWC), dispersion (ϵ), and auto-conversion threshold (T) in fog.

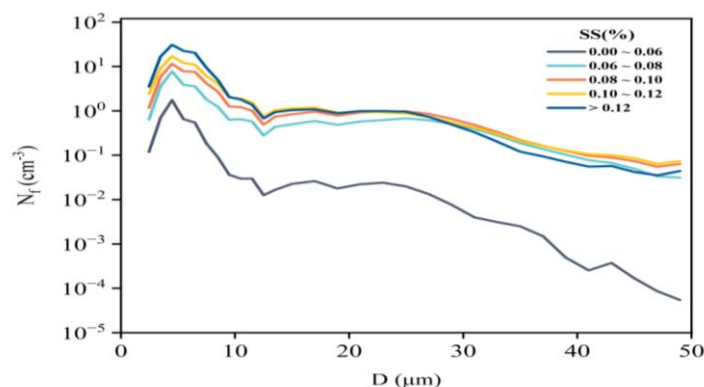


Figure 10: Average spectrum of fog droplets at different supersaturation levels

315 Probability distribution of fog droplet size and concentration for both $\epsilon \leq 0.4$ (Fig. 11a) and $\epsilon > 0.4$ (Fig. 11c) reveals that in the case of $\epsilon > 0.4$, the presence of large droplets ($>12 \mu\text{m}$) in fog significantly increases, and the $N_f(D)$ extends towards the larger droplet end ($>28 \mu\text{m}$). It is shown that, fog droplets are mostly in the small droplet range and primarily grow by condensation with $\epsilon \leq 0.4$ (Fig. 11a). Comparing difference of $\epsilon > 0.4$ and $\epsilon \leq 0.4$ (Fig. 11e), it can be seen that in $\epsilon > 0.4$ (Fig. 11e), the aerosol number concentration and probability is less in the all range compared to $\epsilon \leq 0.4$ (Fig. 11d). In this

320 case, due to the high aerosol concentration, the concentration of activated fog droplets is also high, resulting in a slow growth rate of the droplets and a smaller relative dispersion. This is the reason that, in Fig. 9d, when $\epsilon \leq 0.4$, the ϵ remains essentially constant as the SS increases. This leads to fog droplets primarily distributed in the range of $2 \mu\text{m}$ to $12 \mu\text{m}$, and their growth depends on the condensation process, with limited growth rates. Increasing SS only increases the N_f of fog droplets. When

325 $\epsilon > 0.4$, the $N_f(D)$ of fog droplets larger than $12 \mu\text{m}$ significantly increases. As T increases, although the collision-coalescence process consumes small droplets, the increase in SS still leads to an increase in the number of small droplets. If the number of small fog droplets consumed by the collision-coalescence and condensation process is replenished by the fog droplets generated by the activation process, leading to an increase in ϵ . However, when the SS increases to 0.1% , ϵ starts to decrease. This is because if there are too many small fog droplets, it will result in a decrease in the MVD . What's more, there maybe sedimentation of large droplets with SS larger than 0.12% , leading to a decrease in the ϵ of the fog droplet spectrum. It is

330 shown that SS and aerosols fundamentally affect the magnitude of the T and ϵ .

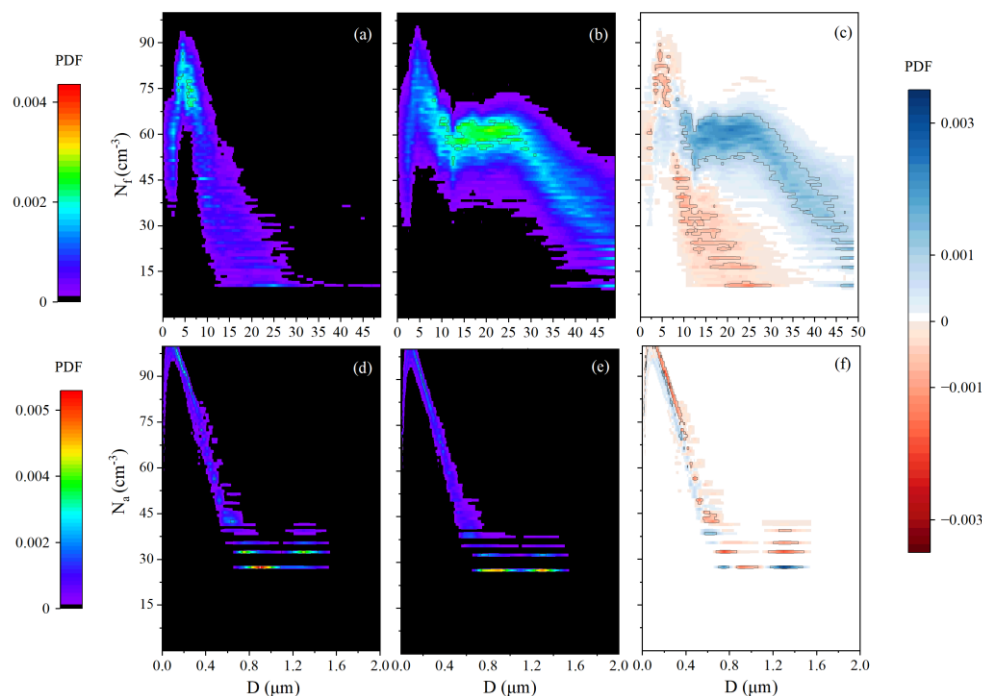


Figure 11 Size and concentration probability density (PDF) diagrams of fog droplet size distribution for (a) $\varepsilon \leq 0.4$; (b) $\varepsilon > 0.4$; (c) difference of $\varepsilon > 0.4$ and $\varepsilon \leq 0.4$ and of aerosol particles size distribution for (d) $\varepsilon \leq 0.4$; (e) $\varepsilon > 0.4$; (f) difference of $\varepsilon > 0.4$ and $\varepsilon \leq 0.4$

335 4 Discussion

This study explores the evolution characteristics of fog microphysics based on 19 fog observation data and found that the relationship between ε and MVD is similar to the findings of Lu et al. (2020), indicating the existence of a critical value for the MVD . Above and below the critical value, the relationship between ε and MVD undergoes changes. It is worth mentioning that in the study by Rui et al. (2022), an increase in the T weakens the negative correlation between ε and MVD , and strengthens the positive correlation. However, in this study, it was found that an increase in the T enhances the negative correlation between ε and MVD . The main reason for the increasing and then converging trend of fog droplet spectrum ε and LWC is that the LWC is easily influenced by fog droplet activation and condensation growth, weakening the negative correlation between ε and LWC . Previous research results have shown that Liu and Daum (2002), Rogers and Yau (1989), Yum and Hudson (2005) used condensation theory to predict a positive correlation between ε and N_f . However, there are also observations indicating a negative correlation between ε and N_f (Yum et al., 2005; Pawlowska et al., 2006; Lu et al., 2007), and the change in ε with increasing N_f is positive or shows a gradually converging trend (Zhao et al. 2006). In this study, both of the above phenomena were observed simultaneously. When T is small and the $N_f(D)$ is narrow, the ε gradually converges with an increasing N_f . When T becomes larger and the $N_f(D)$ widens, the ε shows a positive correlation with the N_f .



350 Therefore, the relationship between ε and N_f needs to be discussed separately based on different situations. The relationship between ε and T as well as SS is more complex. Additionally, the correlation between ε and T and SS depends to some extent on the aerosol size distribution and the number of activated aerosols.

5 Conclusions

In this study, we used the droplet and aerosol particle spectrum data obtained during 19 radiation fog observation experiments
355 conducted in Xishuangbanna in winter 2019 to investigate the evolution patterns and mechanisms of radiation fog microphysical properties in the region and obtain the following conclusions:

(1) There are significant differences in the correlation between various microphysical quantities and the ε under different T values. At T below 0.4, LWC and MVD are positively correlated with ε , mainly due to the dominate condensation and
360 activation of fog droplet. Fog droplet growth primarily depends on the condensation process, leading to ε converging with increasing N_f in this situation. When T is greater than 0.4, there is no significant correlation between LWC and ε , and the effects of fog droplet condensation, coalescence, and activation processes all need to be considered. In this condition, the collision-coalescence and condensation processes are stronger than the activation process, thus MVD is negatively correlated with ε . The active coalescence process tends to widen the $N_f(D)$ towards the larger droplet end, increase N_f , and facilitate an
365 increase in ε , so ε is positively correlated with N_f . Therefore, the strength of the coalescence process has a certain influence on the change rule of the ε .

(2) Increasing the T can increase the MVD and LWC in the fog, and the impact on the N_f is limited by the activation process. The correlation between ε and T is constrained by the N_f in the range of 2 μm to 12 μm of the fog, and they do not have a
370 simple linear relationship. In addition, the quantity of large droplets indirectly reflects the strength of coalescence. More large droplets indicate stronger coalescence, while fewer large droplets indicate weaker coalescence. If both the coalescence process and the activation process are active, it will increase the ε in the fog. Otherwise, a strong coalescence process will result in low ε .

(3) As the SS increases, the N_f of small droplets in the fog also increases, thereby changing the variation of microphysical quantities that affect the ε . In addition, if the initial nucleated $N_f(D)$ is narrow, and the $SS - \varepsilon$ relationship is not obvious, with little change in ε with SS . After the $N_f(D)$ widens, the $SS - \varepsilon$ relationship strengthens, and the ε increases and then decreases with increasing SS . When the SS is greater than 0.12 %, the N_f of droplets in the range of 30 μm to 50 μm decreases, and larger droplets may settle due to gravity, resulting in a decrease in ε with increasing SS .



380

This study is mainly based on observations of fog microphysics, and the reasons for the reduction of larger droplets at high *SS* have not been conclusively determined. Future research should combine numerical simulations to further investigate the underlying mechanisms. Additionally, the findings of this study may also be applicable to inland radiative fog processes in relatively clean areas such as Xishuangbanna in China.

385 **Data availability**

The data are available from the authors upon request.

Author contributions

Xiaoli Liu and Zhenya An shaped the concept of this study and refined the approach during extensive discussions. Zhenya An and Xiaoli Liu carried out the data analysis. Zhenya An prepared the figures and wrote the initial draft, which was subsequently
390 refined by both authors.

Conflict of Interest

The authors declare that the research was conducted in the absence of any commercial or financial relationships that could be construed as a potential conflict of interest.

Acknowledgments

395 In addition, we acknowledge the High Performance Computing Center of Nanjing University of Information Science and Technology for their support of this work.

Funding

This work was supported by the National Natural Science Foundation of China (Grant Nos. 42061134009 and 41975176).

References

400 Anil Kumar, V., Pandithurai, G., Leena, P. P., Dani, K. K., Murugavel, P., Sonbawne, S. M., Patil, R. D., and Maheskumar, R. S.: Investigation of aerosol indirect effects on monsoon clouds using ground-based measurements over a high-altitude site in Western Ghats, *Atmos. Chem. Phys.*, 16, 8423–8430, <https://doi.org/10.5194/acp-16-8423-2016>, 2016.



- 405 Berg, L. K., Berkowitz, C. M., Barnard, J. C., Senum, G., and Springston, S. R.: Observations of the first aerosol indirect effect in shallow cumuli, *Geophys. Res. Lett.*, 38, 809, <https://doi.org/10.1029/2010GL046047>, 2011.
- Chandrakar, K. K., Cantrell, W., and Shaw, R. A.: Influence of turbulent fluctuations on cloud droplet size dispersion and aerosol indirect effects, *J. Atmos. Sci.*, 75, 3191-3209, <https://doi.org/10.1175/JAS-D-18-0006.1>, 2018.
- 410 Desai, N., Glienke, S., Fugal, J., and Shaw, R. A.: Search for microphysical signatures of stochastic condensation in marine boundary layer clouds using airborne digital holography, *J. Geophys. Res. Atmos.*, 124, 2739-2752, <https://doi.org/10.1029/2018JD029033>, 2019.
- Fuzzi S, Facchini M C, Orsi G., Lind, J. A., Wobrock, W., Kessel, M., Maser, R., Jaeschke, W., Enderle, K. H., Berner, A., Scholty, I., Krusiz, C., Reischl, G., Pahl, S., Kaminski, U., Winkler, P., Ogren, J. A., Noone, K. J., Hallberg, A., Fierlinger-Oberlininger, H., Puxbaum, H., Marzorati, A., Hansson, H. -C., Wiedensohler, A., Svenningsson, I. B., Martinsson, B. G., Schell, and D., Georgii, H. W. : The Po valley fog experiment 1989, *Tellus B*, 44, 448-468, <https://doi.org/10.1034/j.1600-0889.1992.t01-4-00002.x>, 1992.
- 420 I. Gulpepe, R. Tardif, S. C. Michaelides, J. Cermak, A. Bott, J. Bendix, M. D. Müller, M. Pagowski, B. Hansen, G. Ellrod, W. Jacobs, G. Toth and S. G. Cober: Fog research: A review of past achievements and future perspectives, *Pure. Appl. Geophys.*, 164, 1121-1159, <https://doi.org/10.1007/s00024-007-0211-x>, 2007.
- Li, Z.: Study of fog in China over the past 40 years, *Acta Meteorol. Sin.*, 59, 616–624, doi: 10.11676/qxxb2001.065 ,2001. (in Chinese)
- 425
- Liu, Y.: Daum P H. Indirect warming effect from dispersion forcing, *Nature*, 419, 580-581, <https://doi.org/10.1038/419580a>, 2002.
- 430 Liu, Y., Daum, P. H., and McGraw, R.: An analytical expression for predicting the critical radius in the autoconversion parameterization, *Geophys. Res. Lett.*, 31, 121, <https://doi.org/10.1029/2003GL019117>, 2004.
- Liu, Y., Daum, P. H., and McGraw, R. L.: Size truncation effect, threshold behavior, and a new type of autoconversion parameterization, *Geophys. Res. Lett.*, 32, 811, <https://doi.org/10.1029/2005GL022636>, 2005.
- 435



- Liu, Y., Daum, P. H., McGraw, R., and Miller, M.: Generalized threshold function accounting for effect of relative dispersion on threshold behavior of autoconversion process, *Geophys. Res. Lett.*, 33, 804, <https://doi.org/10.1029/2005GL025500>, 2006.
- 440 Lu, M. L., Conant, W. C., Jonsson, H. H., Varutbangkul, V., Flagan, R. C., and Seinfeld, J. H.: The marine stratus/stratocumulus experiment (MASE): Aerosol-cloud relationships in marine stratocumulus, *J. Geophys. Res: Atmos.*, 112, D10209, <https://doi.org/10.1029/2006JD007985>, 2007.
- Liu, Y., Daum, P. H., Guo, H., and Peng, Y.: Dispersion bias, dispersion effect, and the aerosol–cloud conundrum, *Environ. Res. Lett.*, 2008, 3, 045021, doi: 10.1088/1748-9326/3/4/045021, 2008.
- 445
- Lu, C., Niu, S., Liu, Y., and Vogelmann, A. M.: Empirical relationship between entrainment rate and microphysics in cumulus clouds, *Geophys. Res. Lett.*, 40, 2333-2338, <https://doi.org/10.1002/grl.50445>, 2013.
- 450 Lu, C., Liu, Y., Yum S S., Chen, J., Zhu, L., Gao, S., Yin, Y., Jia, X., and Wang, Y.: Reconciling contrasting relationships between relative dispersion and volume-mean radius of cloud droplet size distributions, *J. Geophys. Res.: Atmos.*, 125, e2019JD031868, <https://doi.org/10.1029/2019JD031868>, 2020.
- Lu C, Xue Y, Zhu L, and Xu, X.: Evaluation of aerosol indirect effect based on aircraft observations of stratocumulus, *Trans. Atmos. Sci.*, 44, 279-289, doi: 10.13878/j.cnki.dqkxxb.20200613001, 2021. (in Chinese)
- 455
- Musk L F: The fog hazard, *Highway meteorology*. CRC Press, 91-130, <https://doi.org/10.4324/9780203473498>, 1991.
- Martins J A., and Dias M A F S.: The impact of smoke from forest fires on the spectral dispersion of cloud droplet size distributions in the Amazonian region, *Environ. Res. Lett.*, 4, 015002, doi: 10.1088/1748-9326/4/1/015002, 2009.
- 460
- Mazoyer, M., Burnet, F., Denjean, C., Roberts, G. C., Haeffelin, M., Dupont, J. C., and Elias, T.: Experimental study of the aerosol impact on fog microphysics, *Atmos. Chem. Physics.*, 19, 4323-4344, <https://doi.org/10.5194/acp-19-4323-2019>, 2019, 2019.
- 465
- Niu, S., Lu, C., Yu, H., Zhao, L., and Lü, J.: Fog research in China: An overview, *Adv. Atmos. Sci.*, 27, 639-662, <https://doi.org/10.1007/s00376-009-8174-8>, 2010.



- Okita T: Observations of the vertical structure of a stratus cloud and radiation fogs in relation to the mechanism of drizzle formation, *Tellus*, 14, 310-322, <https://doi.org/10.1111/j.2153-3490.1962.tb01342.x>, 1962.
- 470
- Pilié, R. J., Mack, E. J., Kocmond, W. C., Eadie, W. J., and Rogers, C. W.: The life cycle of valley fog. Part II: Fog microphysics, *J. Appl. Meteorol. Climatol.*, 14, 364-374, [https://doi.org/10.1175/1520-0450\(1975\)014<0364:TLCOVF>2.0.CO;2](https://doi.org/10.1175/1520-0450(1975)014<0364:TLCOVF>2.0.CO;2), 1975.
- 475
- Pawlowska, H., Grabowski, W. W., and Brenguier, J. L.: Observations of the width of cloud droplet spectra in stratocumulus, *Geophys. Res. Lett.*, 33, 810, <https://doi.org/10.1029/2006GL026841>, 2006.
- Pöschl, U., Martin, S. T., Sinha, B., Chen, Q., Gunthe, S. S., Huffman, J. A., Borrmann, S., Farmer, D. K., Garland, R. M., Helas, G., Jimenez, J. L., King, S. M., Manzi, A., Mikhailov, E., Pauliquevis, T., Petters, M., D., Roldin, P., Schneider, J., Su, H., Zorn, S. R., Artaxo, P and Andreae, M. O. : Rainforest aerosols as biogenic nuclei of clouds and precipitation in the Amazon, *Sci*, 329, 1513-1516, doi: 10.1126/science.1191056, 2010.
- 480
- Rogers, R., and Yau, M. K.: A short course in cloud physics. 3rd ed. Burlington, MA, USA: Butterworth Heinemann. 1989.
- 485
- Rui, X., Lu, C., Zhu, L., Wang, Y, Yin, Y., and Chen, K.: Effects of cloud microphysical processes on cloud droplet spectral relative dispersion on Mount Huangshan, *Trans. Atmos. Sci.*, 45, 630-640, doi: 10.13878/j.cnki.dqkxxb.20210318003 ,2022 (in Chinese)
- 490
- Spiegel, J. K., Zieger, P., Bukowiecki, N., Hammer, E., Weingartner, E., and Eugster, W.: Evaluating the capabilities and uncertainties of droplet measurements for the fog droplet spectrometer (FM-100), *Atmos. Meas. Tech.*, 5, 2237-2260, <https://doi.org/10.5194/amt-5-2237-2012>, 2012.
- Seinfeld, J. H., and Pandis, S. N.: Atmospheric chemistry and physics: from air pollution to climate change, John Wiley and Sons, 2016.
- 495
- Shen, C., Zhao, C., Ma, N., Tao, J., Zhao, G., Yu, Y., and Kuang, Y.: Method to estimate water vapor supersaturation in the ambient activation process using aerosol and droplet measurement data, *J. Geophys. Res-Atmos*, 123, 10,606-10,619, <https://doi.org/10.1029/2018JD028315>, 2018.
- 500
- Taylor, G. I.: The formation of fog and mist, *Q. J. Roy. Meteor. Soc.*, 43, 241-268, <https://doi.org/10.1002/qj.49704318302> , 1917.



505 Wang, J., Daum P. H., Yum, S. S., Liu, Y., Senum, G. I., Lklu, M. L., and Seinfeld, J. H., Jonsson, H.: Observations of marine stratocumulus microphysics and implications for processes controlling droplet spectra: Results from the Marine Stratus/Stratocumulus Experiment, *J. Geophys. Res.*, 114, D18210, <https://doi.org/10.1029/2008JD011035>, 2009.

510 Wang, Y., Niu, S., Lu, C., Lv, J., Zhang, J., Zhang, H., Zhang, S., Shao, N., Sun, W., Jin, Y. and Song Q.: Observational study of the physical and chemical characteristics of the winter radiation fog in the tropical rainforest in Xishuangbanna, China, *Sci. China Earth Sci.*, 64, 1982-1995, <https://doi.org/10.1007/s11430-020-9766-4>, 2021.

515 Wang, Y., Lu, C., Niu, S., Lv, J., Jia, X., Xu, X., Xue, Y., Zhu, L., and Yan, S.: Diverse dispersion effects and parameterization of relative dispersion in urban fog in eastern China, *J. Geophys. Res-Atmos.*, e2022JD037514, <https://doi.org/10.1029/2022JD037514>, 2023.

Xu F, Niu S, Zhang Y, zhao, L., Yue, Y., Liu, L., Cai, S., and Zhang, S.: Climatic characteristics of fog in Leizhou Peninsula and the mechanism of production and elimination, *Trans. Atmos. Sci.*, 34, 423-432, doi: 10.13878/j.cnki.dqkxxb.2011.04.008., 2011. (in Chinese)

520 Yang, Z., S. Xu, and B. Geng: The formation mechanism and microphysical structure of spring fog in Zhoushan area, *Acta Oceanol. Sin.*, 11, 431-438, 1989.

525 Yum, S., and Hudson, J. G.: Adiabatic predictions and observations of cloud droplet spectral broadness, *Atmos. Res.*, 73, 203-223, <https://doi.org/10.1016/j.atmosres.2004.10.006>, 2005.

Yang, J., Chen, B., Chen, B., Yin, Y.: *Physics of Clouds and Precipitation*, Beijing: Meteorological Press, 92-93, 2011.

530 Yang, J., Gao, Y., Wu, B., Dong, Q., Wang, Z., and Hu, H.: A study of the stratospheric fog process in Tianjin and its airborne microphysical characteristics in individual cases, *Trans. Atmos. Sci.*, 44, 945-953, doi: 10.13878/j.cnki.dqkxxb.20200516012, 2021. (in Chinese)

Zhao, C., Tie, X., Brasseur, G., Noone, K. J., Nakajima, T., Zhang, Q., Zhang, R., Huang, M., Duan, Y., Li, G., and Ishizaka, Y.: Aircraft measurements of cloud droplet spectral dispersion and implications for indirect aerosol radiative forcing, *Geophys. Res. Lett.*, 33, 809, <https://doi.org/10.1029/2006GL026653>, 2006.